

White paper

The clinical usefulness of S-Fusion™ for Prostate

Dirk Clevert, MD

Radiology, LMU Munich, Germany

Introduction

Prostate cancer is the most common cancer in men in Germany with an incidence of about 65,000 new cases per year [1].

Among the causes of death related to malignancies, prostate cancer is in third place. More than 13,000 men died of prostate cancer 2011 in Germany [1].

The risk of developing clinically significant prostate cancer depends on age. The ten-year risk of developing the disease is < 0.1% for a 35-year-old man, while the risk for a 75-year-old man is just under 6% [1]. Overall, the lifetime risk for the disease is about 13%, the lifetime mortality risk is 3.3% [1].

The increased life expectancy of the population and the improved diagnosis of prostate cancer, are the reason why the disease increased. In particular, the use of prostate-specific antigen (PSA) as a tumor marker has significantly increased the incidence [2].

The initial determination of the PSA value and the digital-rectal examination provide in many cases an initial indication of the presence of pathological changes in the prostate. If the findings are positive, the recommendations of the S3 guideline are, that the patient should undergo a 10 to 12-fold assisted prostate biopsy under transrectal ultrasound control [3].

With the help of this biopsy technique, however, 19-52% of all tumors can be missed and their aggressiveness can be underestimated in comparison to the pathological findings (radical prostatectomy) or better biopsy methods (32- 50%) [4-7].

However, with increasing improvements in diagnostics, we will also detect low-risk tumors, which will not affect the survival of patient [8, 9].

With early targeted detection, prostate cancer can usually be detected at a localized stage [10], so that the patient has several treatment options to choose from. These range from active monitoring or focal therapy to an established curative therapy, e.g. radical prostatectomy and/or radiotherapy [11, 12].

Conventional ultrasound imaging

Conventional transrectal ultrasound (TRUS) is the most commonly used urological imaging technique for assessing the prostate. TRUS is ideal for volume determination and facilitates the performance of randomized prostate biopsies. However, the conventional transrectal ultrasound has some limitation in detecting prostate carcinoma, since carcinoma foci are often low-echo, but can also be isoechogenic or hyperechogenic [13, 14] (Fig. 1-2).

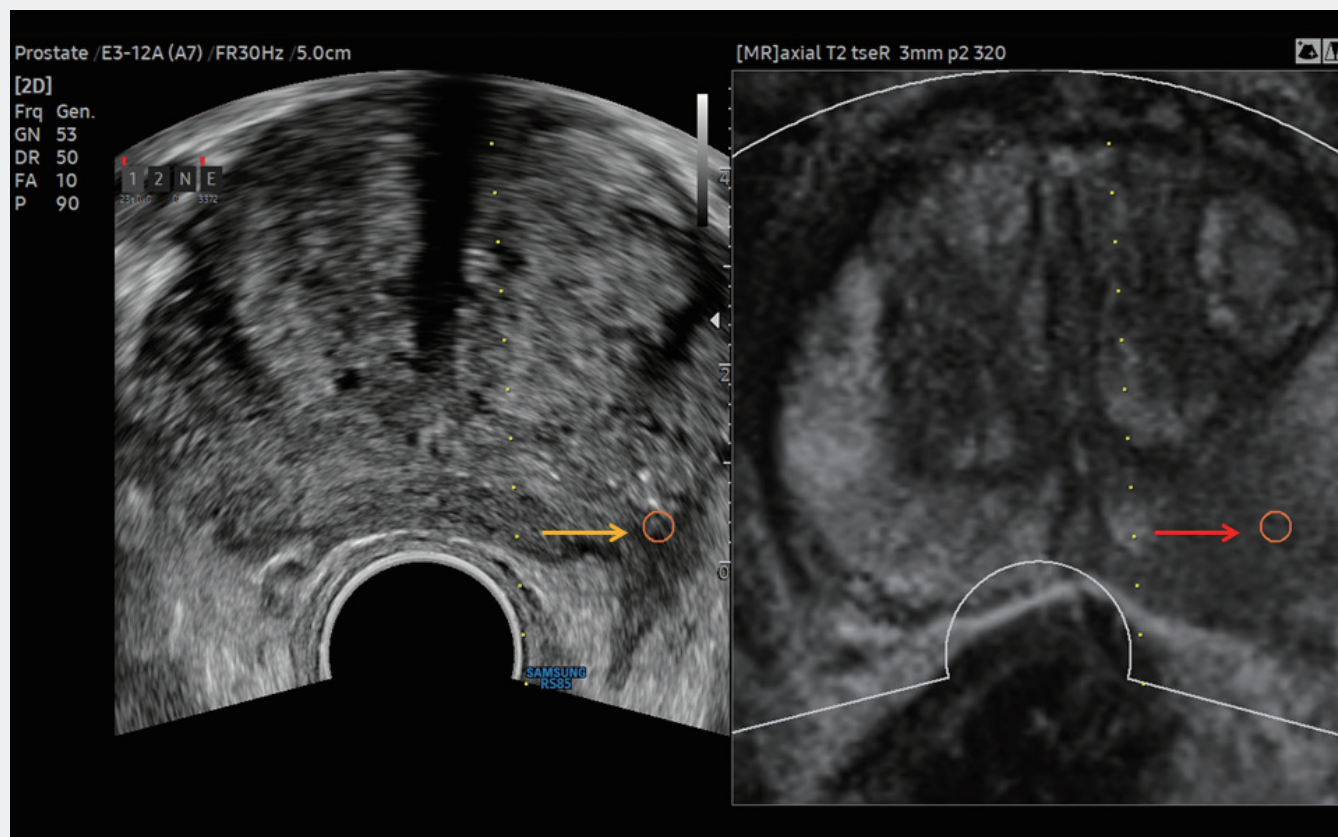


Figure 1. Image fusion of the prostate: Suspected small low-echo lesion (yellow arrow) of the prostate in conventional B-image sonography and in MRI imaging a signal-lowered (hypointense) carcinoma suspected lesion in the peripheral zone on the left (red arrow). In the registered MRI image fusion, the prostate is recorded in the axial MRI plane.

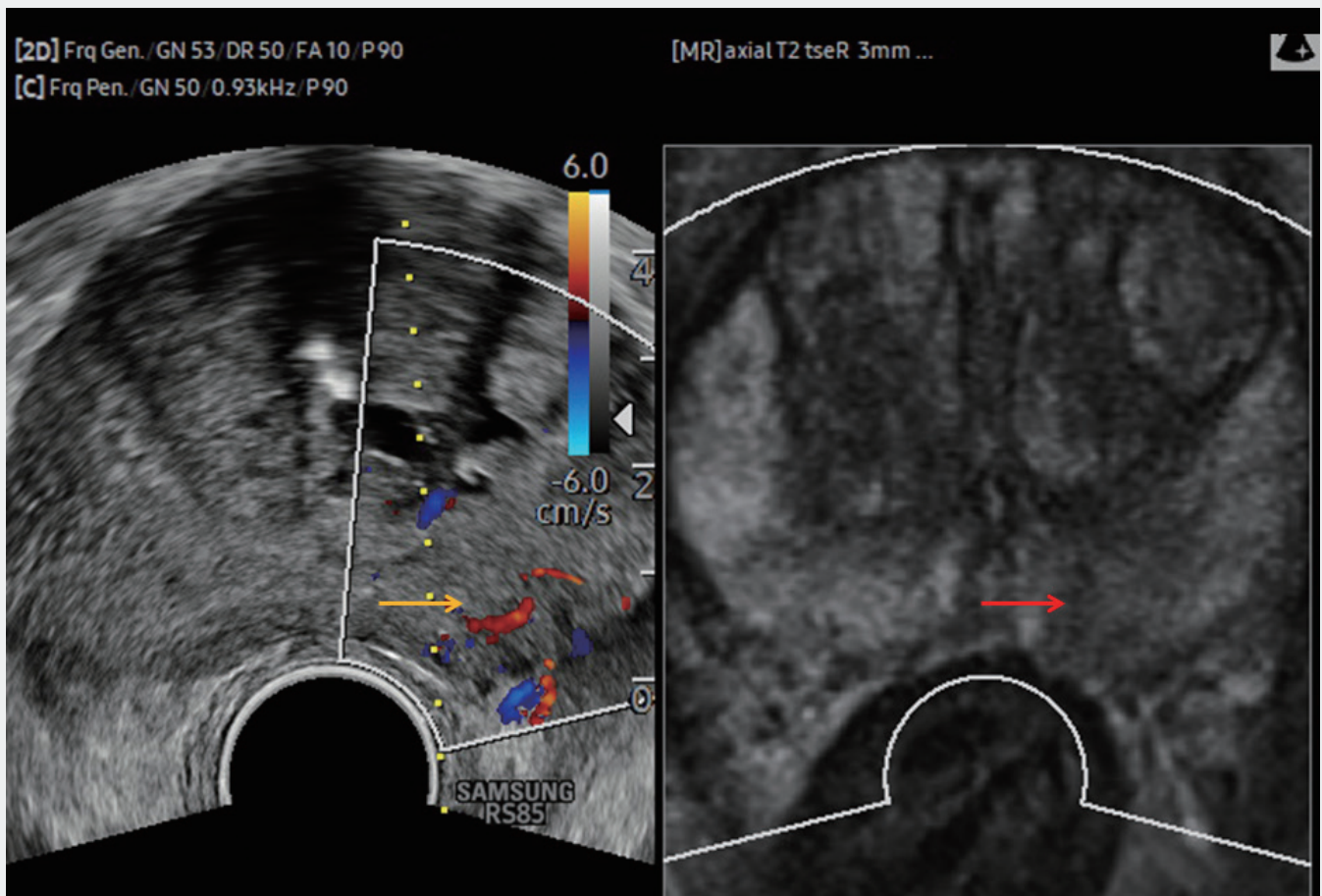


Figure 2. MRI-ultrasound fusion of the prostate. Color-coded duplex sonography shows the superficial lesion with increased vascularization (yellow arrow). The left T2-weighted MRI image shows a signal-lowered (hypointense) lesion suspected of being carcinomatous (red arrow).

This circumstance and the great dependence of the investigator examination [15] are probably the reason for the sometimes very contradictory results of the published studies. For example, the percentage of proven malignancy for low-echo lesions is given from 18 - 57% [16]. The sensitivity in these studies varies between 15 - 96 %, the specificity between 46 - 93 % [17-19]

Due to the limitations of conventional prostate ultrasound biopsy, a systematic biopsy will be used in contrast to targeted biopsy of other solid organs.

Multiparametric magnetic resonance imaging (MRI) of the prostate:

Multiparametric MRI (mpMRI) is currently the leading imaging method for the detection and characterization of prostate cancer with a high diagnostic value. Especially in patients with previous negative TRUS biopsy and persistent suspected cancer MRI will be used [20-21].

Today, multiparametric MRI combines anatomical and functional data acquisition. The examination includes mainly of morphological T2-weighted imaging (T2w), diffusion weighted imaging (DWI) and dynamic contrast enhanced imaging (DCEMRI) [22].

The advantage of MRI imaging is the variety of image contrasts, which allows structural imaging and the assessment of different aspects of healthy and pathologically altered tissue. The high resolution T2w sequences are important for morphological imaging of the prostate because they provide the best representation of the zonal prostate anatomy and the capsule and allow assessment of tumor extension, especially extraprostatic growth [22-23].

For this reason, mpMRI can help to make the surgical decision for or against preservation of the neurovascular bundles prior to a planned radical prostatectomy [24-26].

Since 2012 guidelines are available for reporting MRI-findings [27]. PI-RADS (“prostate imaging-reporting and data system”) classify individual lesions and summarize the findings according to a 5-point scale (Table 1).

Table 1. PI-RADS (Prostate Imaging Reporting and Data System) score: Definition of risk categories.

	Meaning
PI-RADS 1	Very low (clinically significant cancer highly unlikely)
PI-RADS 2	Low (clinically significant cancer unlikely)
PI-RADS 3	Intermediate (clinically significant cancer equivocal)
PI-RADS 4	High (clinically significant cancer likely)
PI-RADS 5	Very high (clinically significant cancer highly likely)

MRI-fusion biopsy

In our daily setting we are using the Samsung RS85 V2.0 ultrasound system (Samsung Medison Co., Ltd) for prostate fusion.

In order to be able to perform MRI-ultrasound guided biopsy on patients who have been diagnosed with suspicious findings in an MRI examination, a so-called image fusion technique could be used. In this procedure ultrasound image and MRI images will be used and fused in real time (Fig.3). In addition to a systematic biopsy, this image fusion can be used to biopsy suspect areas in MRI imaging [28].

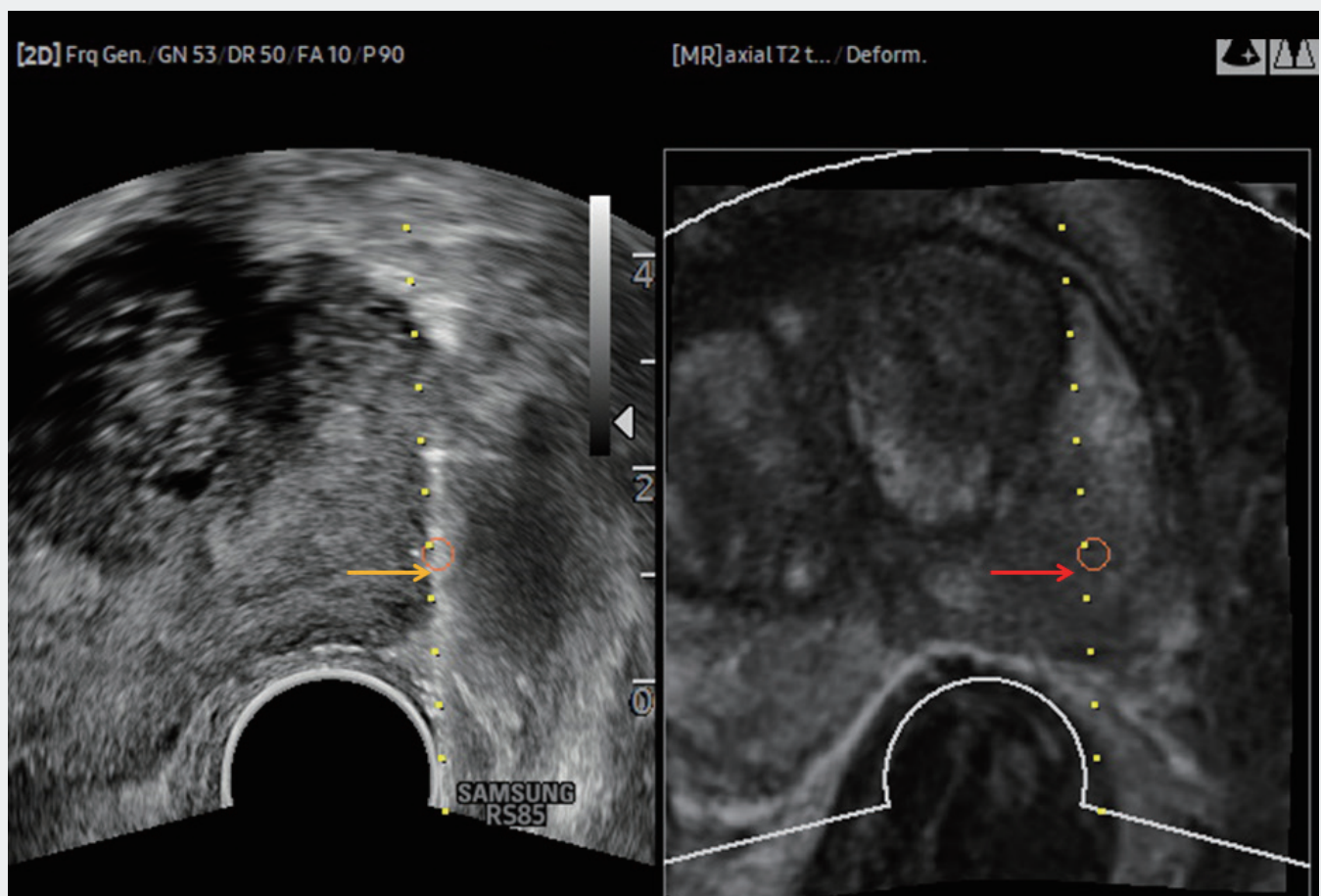


Figure 3. The targeted MR ultrasound fusion biopsy (red and yellow arrows) revealed an acinar adenocarcinoma of the prostate (Gleason 3+4=7a).

For this image fusion technic a magnetic field generator, a corresponding transducer and patient sensor are required as hardware. In addition, suitable software must be installed on the ultrasound device. The transducer and patient sensor will be detected by a magnetic positioning system and the exact position of the sensor in examination room is calculated. For image fusion, DICOM data sets of all common cross sectional imaging techniques can be used. The DICOM data are loaded into the ultrasound system and the data sets will be registered in a second step. This image registration can either be performed manual or automatically based on or plane or volume imaging [29-31].

After a successful image fusion, the registered MRI images move simultaneously to the ultrasound plane. Optionally, the registered images can be viewed either in the overlay technique or in the side-by-side view. Conventional ultrasound tools such as color Doppler, Power Doppler or contrast-enhanced ultrasound can be integrated into the merged image [32-34].

After starting the prostate software **anauto** calibration algorithm is on the system available, this feature improve the detecting of the prostate shape and calculate automatically the prostate volume (Fig. 4). Additionally minor or major adaptation could be done manually (Fig. 5).

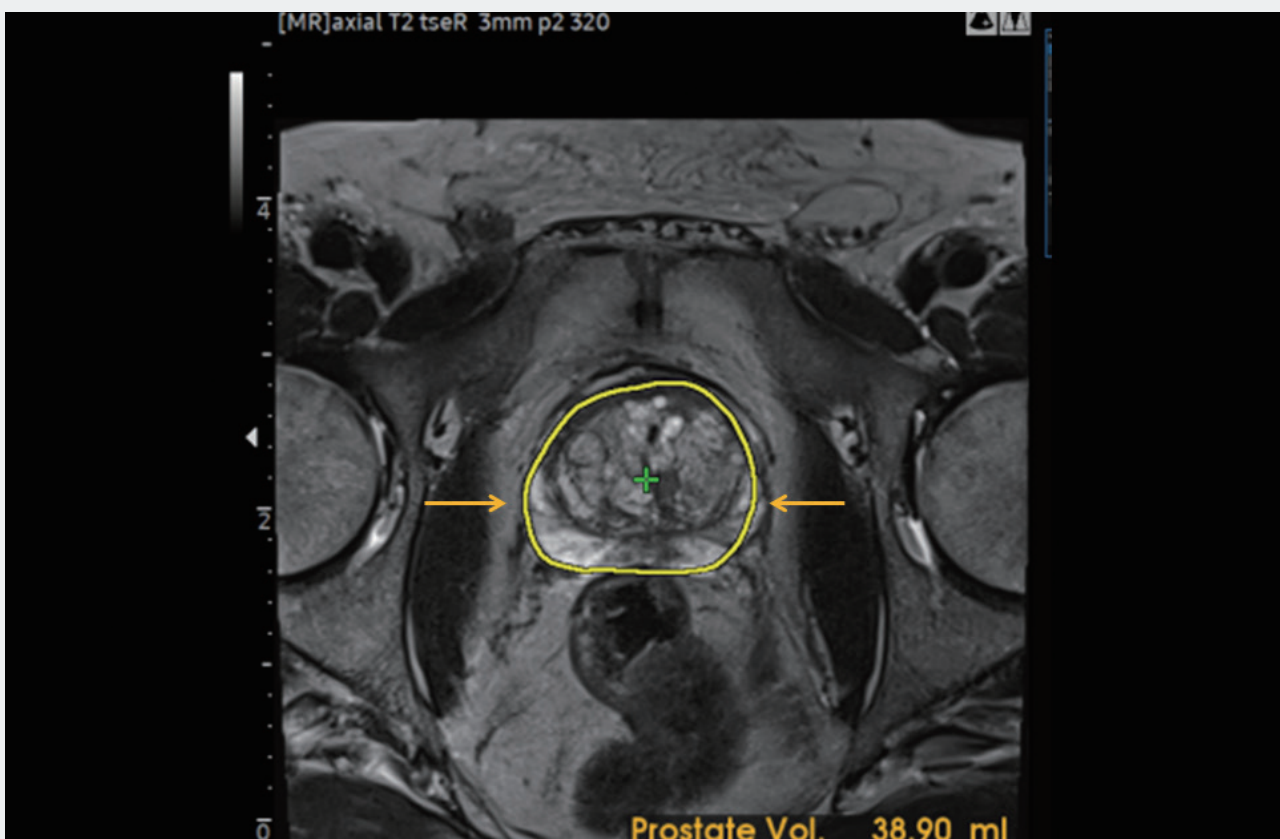


Figure 4. Auto calibration algorithm improves the detecting of the prostate shape (yellow arrows) and calculates automatically the prostate volume (38.90 ml).

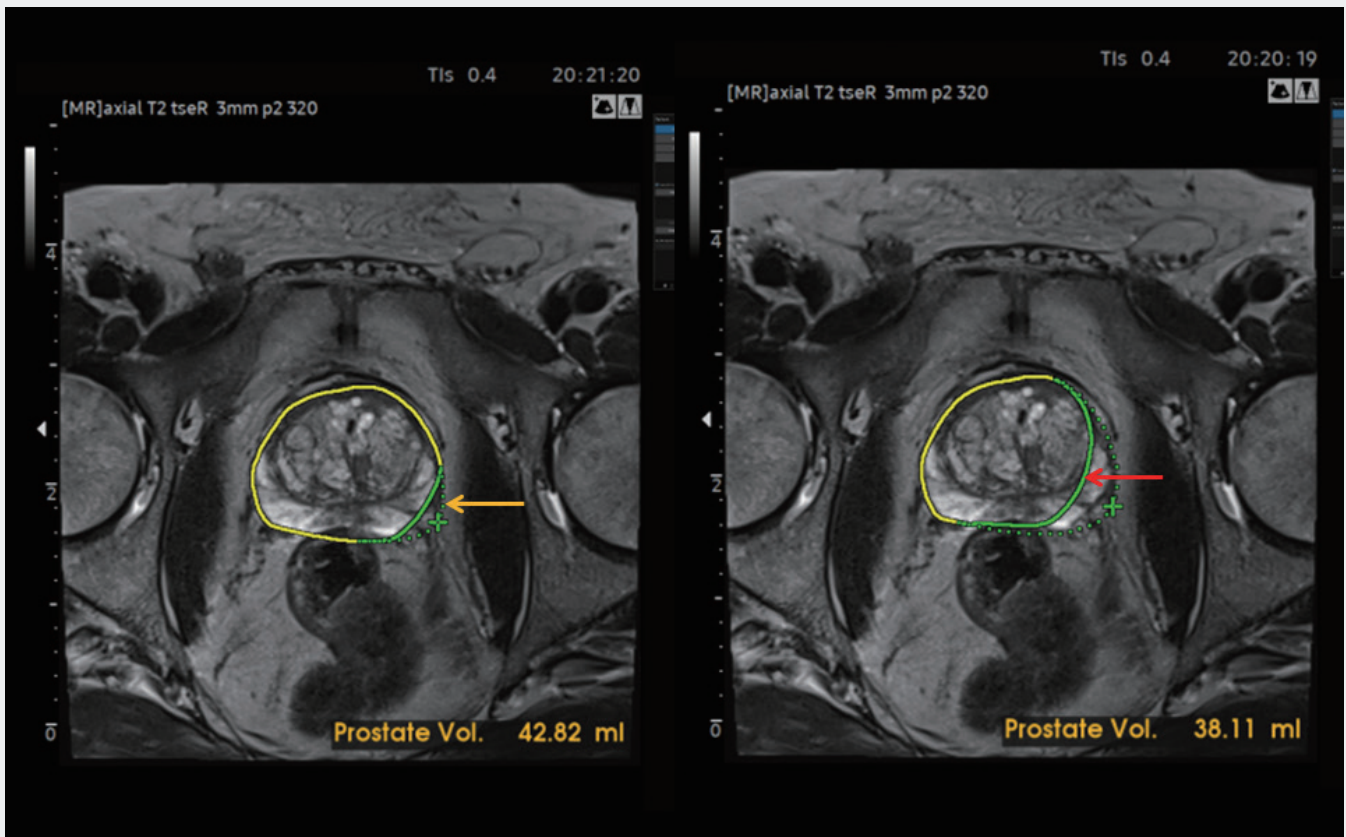


Figure 5. Additionally minor (yellow arrow) or major (red arrow) adaptation could be done manually to calculate the prostate volume.

On the system a deformation correction algorithm could be used, this is a feature to improve the accuracy of registration by correcting deformed prostate shape when transducer is compressed the tissue during the procedure and it could be useful for targeted biopsy procedure (Fig. 6-9).

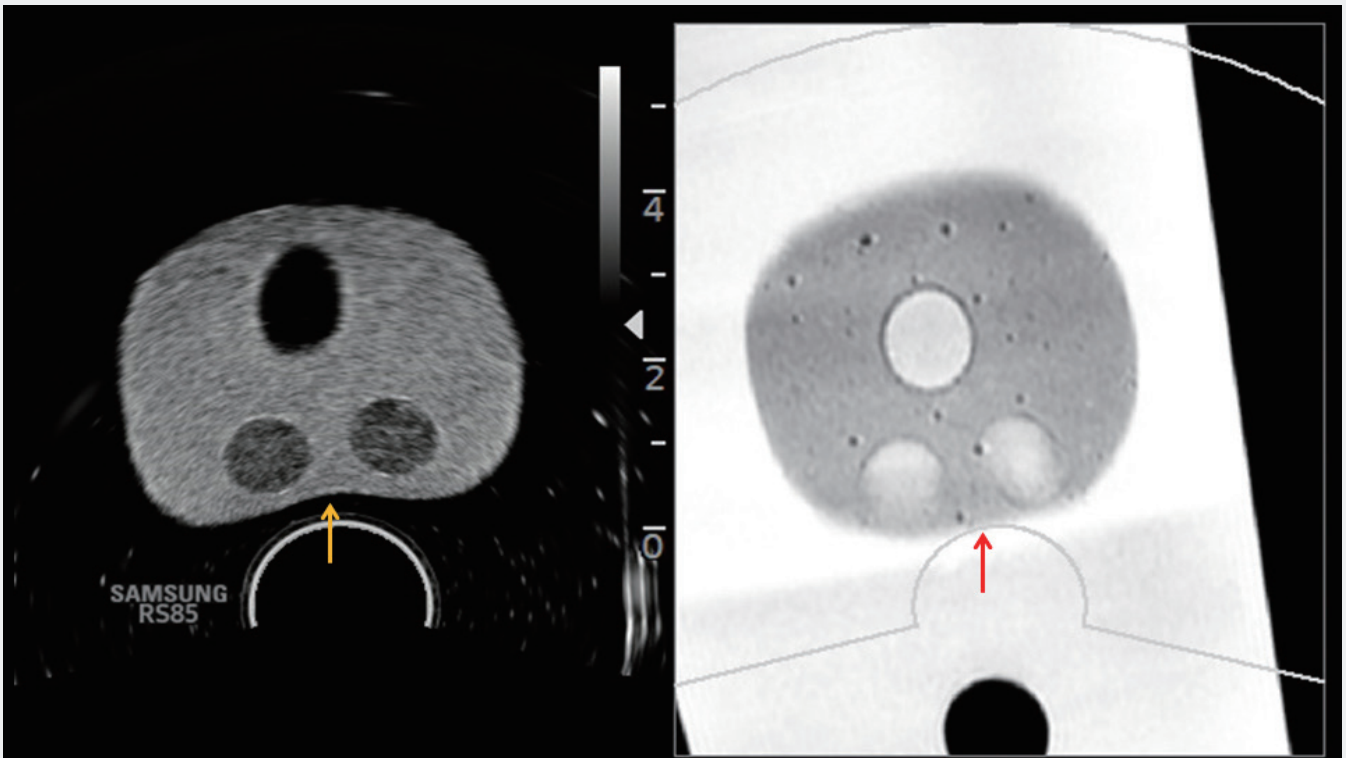


Figure 6. During the examination the probe compressed the prostate tissue (yellow arrow) and the result is a deformation of the prostate and a mismatch between ultrasound and MRI data (red arrow).

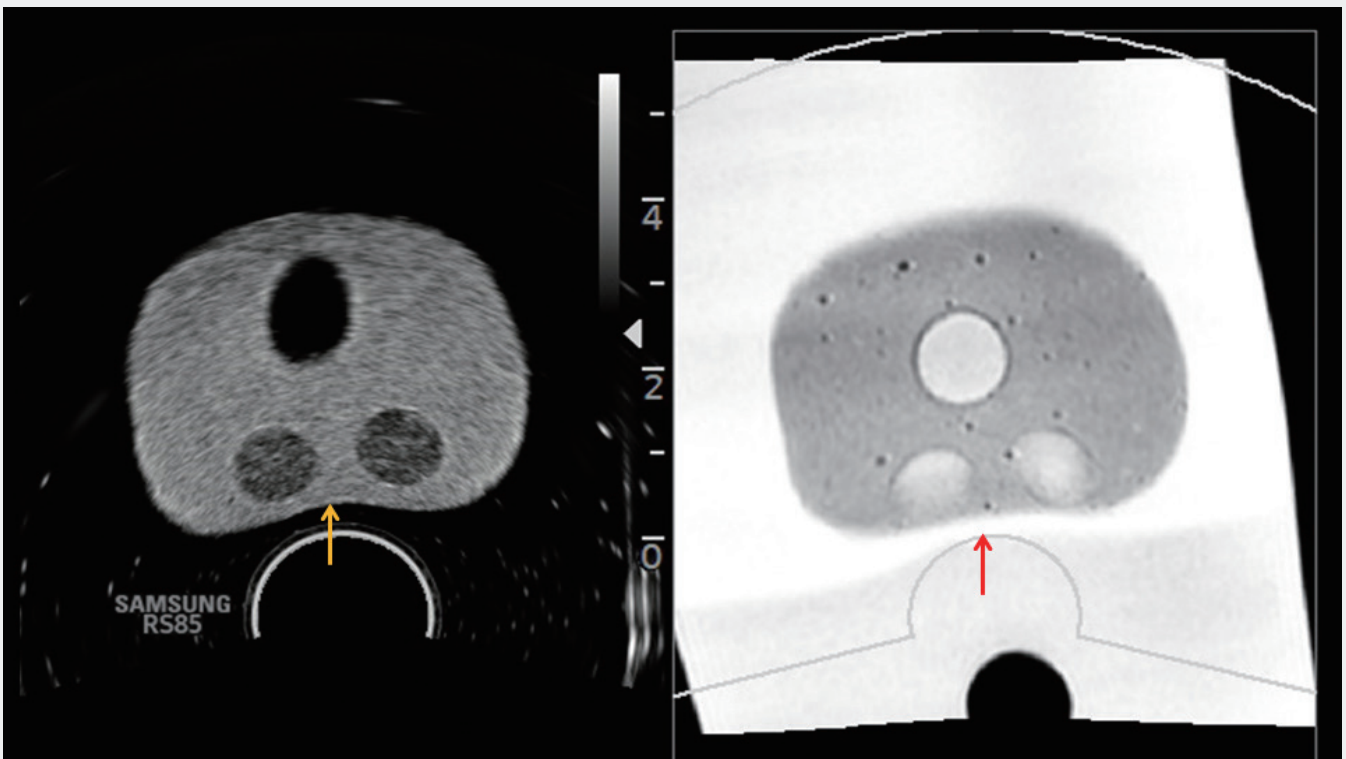


Figure 7. The deformation correction algorithm on the system could be used to improve the accuracy of registration by correcting deformed prostate MRI shape (red arrow) when transducer is compressed the tissue (yellow arrow) during the procedure.

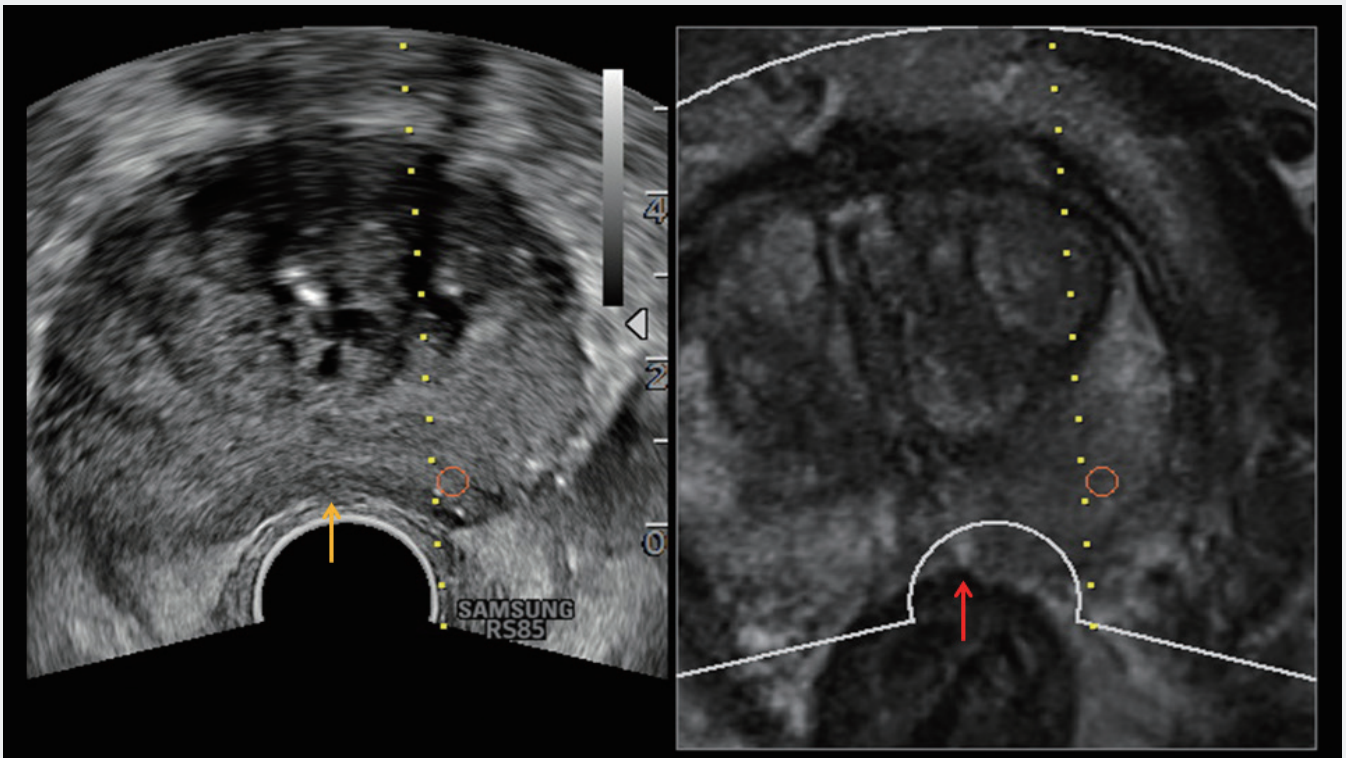


Figure 8. During the examination the probe compressed the prostate tissue (yellow arrow) there is now a mismatch between the location of the prostate and the shape of the prostate in the MRI-image (red arrow).

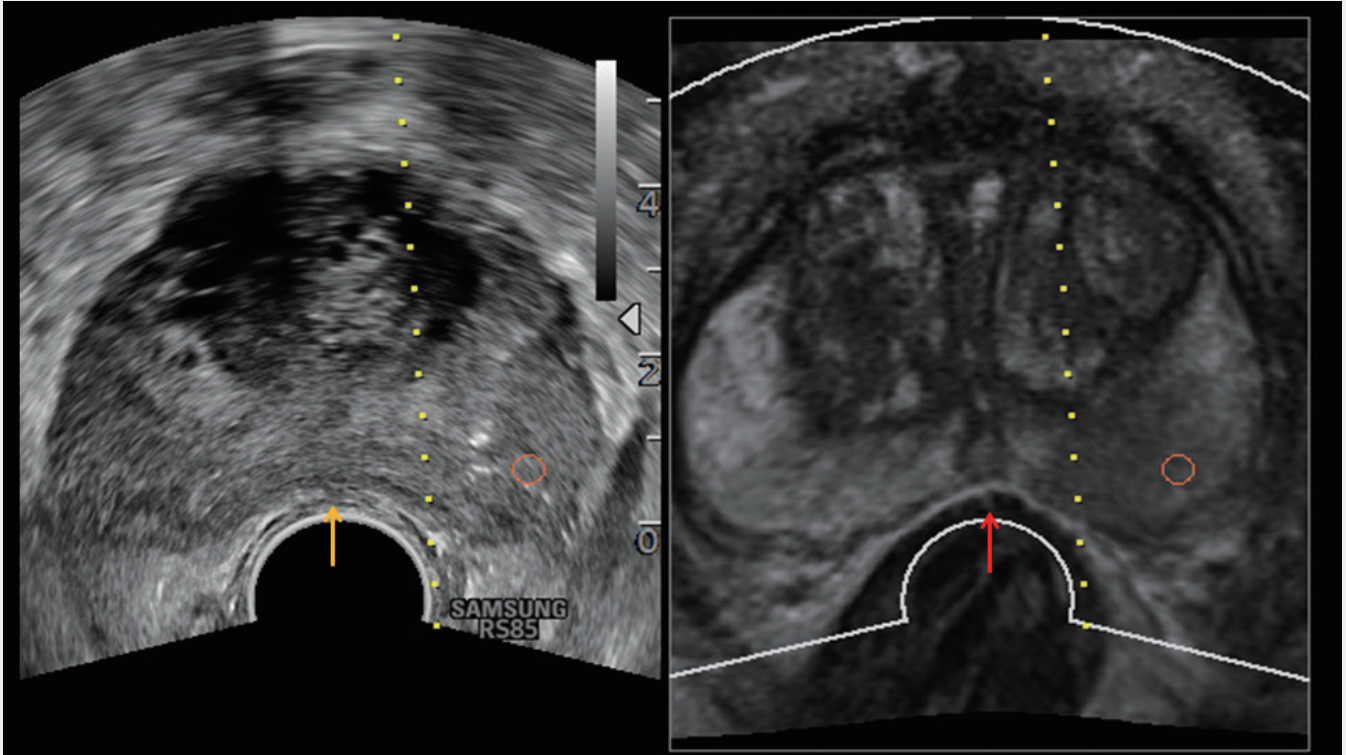


Figure 9. Same patient as Figure 8. The deformation correction algorithm on the system improve the accuracy of registration by correcting the deformed prostate MRI shape (red arrow) when transducer is compressed the prostate tissue (yellow arrow).

In order to compensate a possible movement of the patient, a patient tracker is available which allows the patient to be repositioned during the intervention without having to re-register the MRI data.

The registration of ultrasound and MRI images in image fusion improves spatial orientation and suspicious focal findings can be better detected and biopsied in a targeted manner. In addition, this method allows an assessment of microvascularization in direct comparison to sectional imaging [35-37].

In clinical routine, this technique can be used for fusion biopsy of the prostate or after prostate intervention [38-43].

It takes less than 10 minutes to load the MRI data into the ultrasound system, register and perform the biopsy. During registration, the volume of the prostate is also automatically determined and the biopsy taken can be displayed in the 3D MRI data set. By using the auto calibration on the S-Fusion™ for prostate it supports a real-time auto calibration function that helps to perform more accurate and reliable procedures. The 3D modeling for prostate allows safe navigation and precise targeting during prostate biopsies created from MR data sets, and also provides a function to report the biopsy location in the volume (Fig. 10-14).

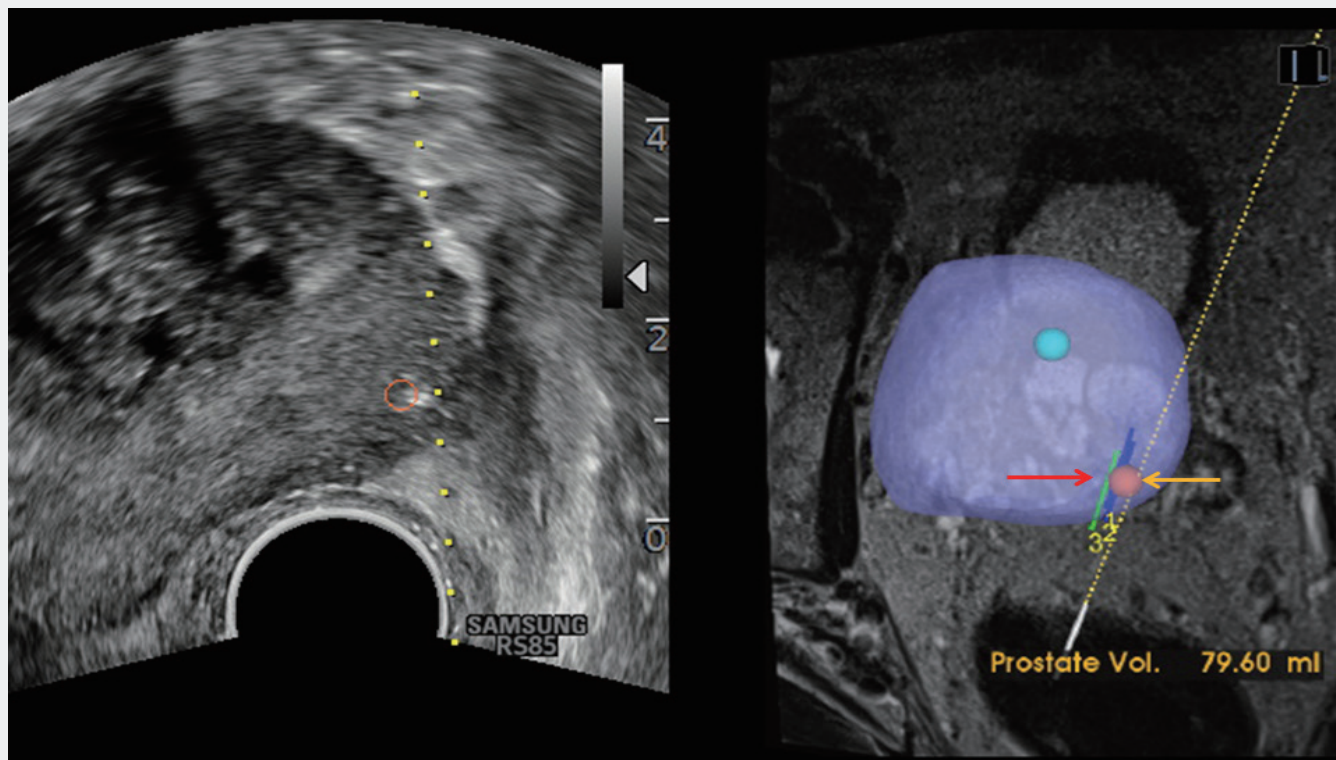


Figure 10. The 3D modeling for prostate allows precise targeting during prostate biopsies based on the created data sets from MRI. It also provides a function to report biopsy location. Target lesion marked as a red sphere (yellow arrow) the already done biopsies are reported in the prostate model (red arrow).

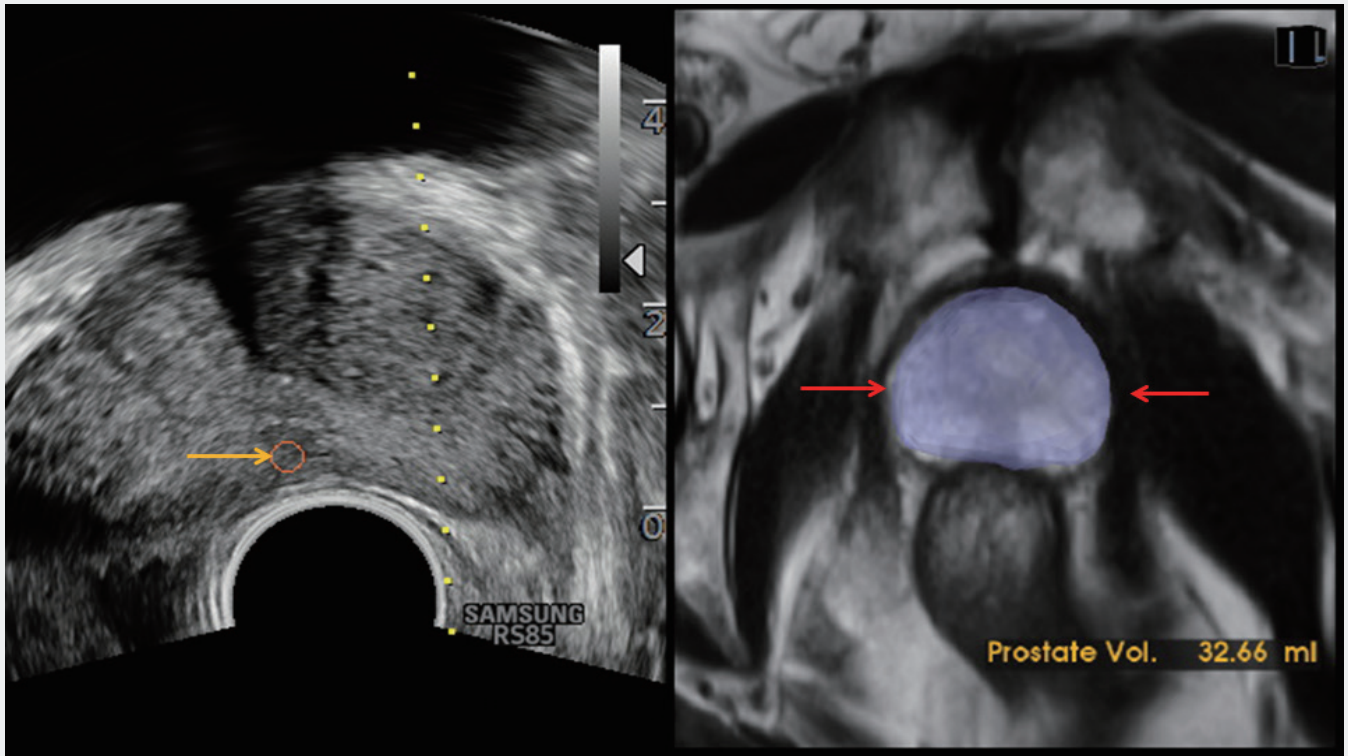


Figure 11. S-Fusion™ auto calibration for prostate supports a real-time auto calibration function that helps to perform more accurate and reliable procedures. The system automatically detects the shape of the prostate (red arrows) and measure the prostate volume (32.6 ml). The target lesion is already detected in conventional B-image (yellow arrow).

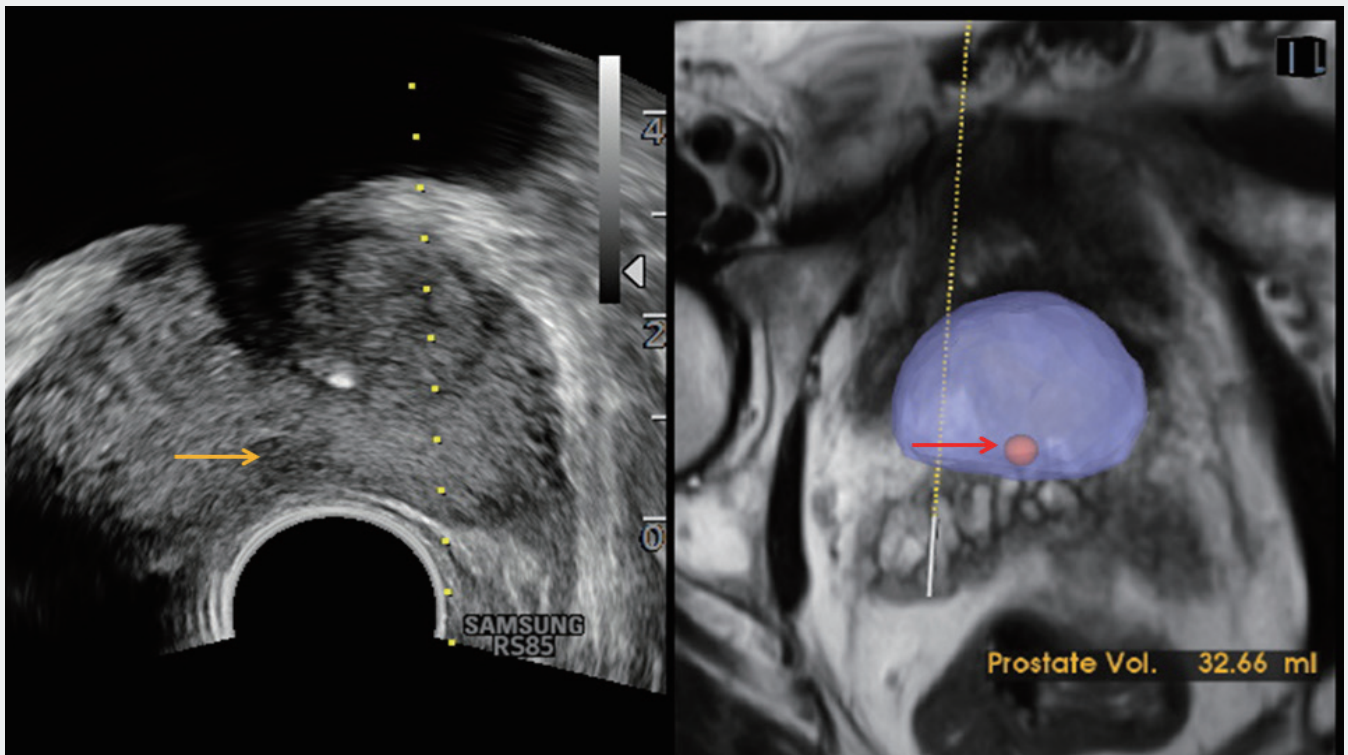


Figure 12. S-Fusion™ transfer the target lesion detected in conventional B-image (yellow arrow) into the 3D volume (red arrow). Additionally the prostate volume (32.6ml) is still visible during intervention.

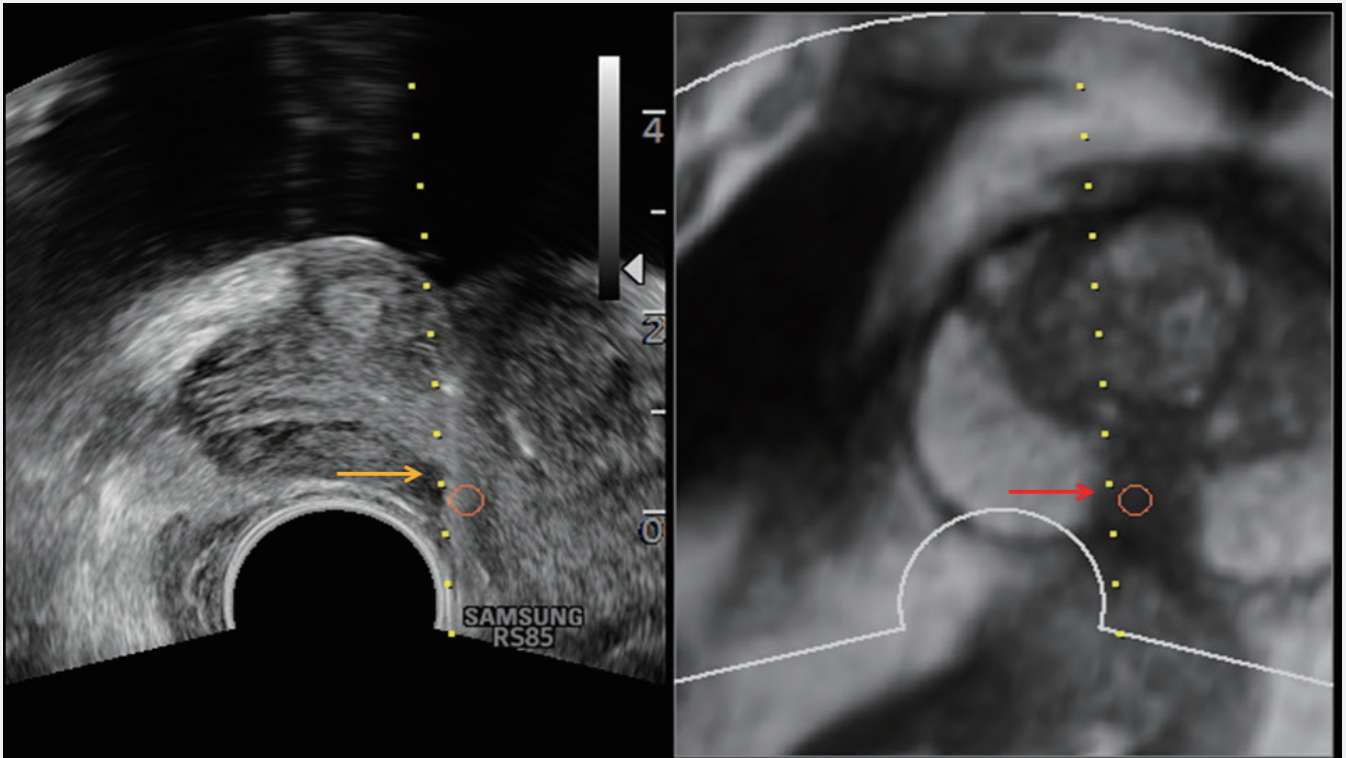


Figure 13. The targeted MR ultrasound fusion biopsy (red and yellow arrows) revealed poor differentiated acinar prostate carcinoma (Gleason 4+4 = 8).

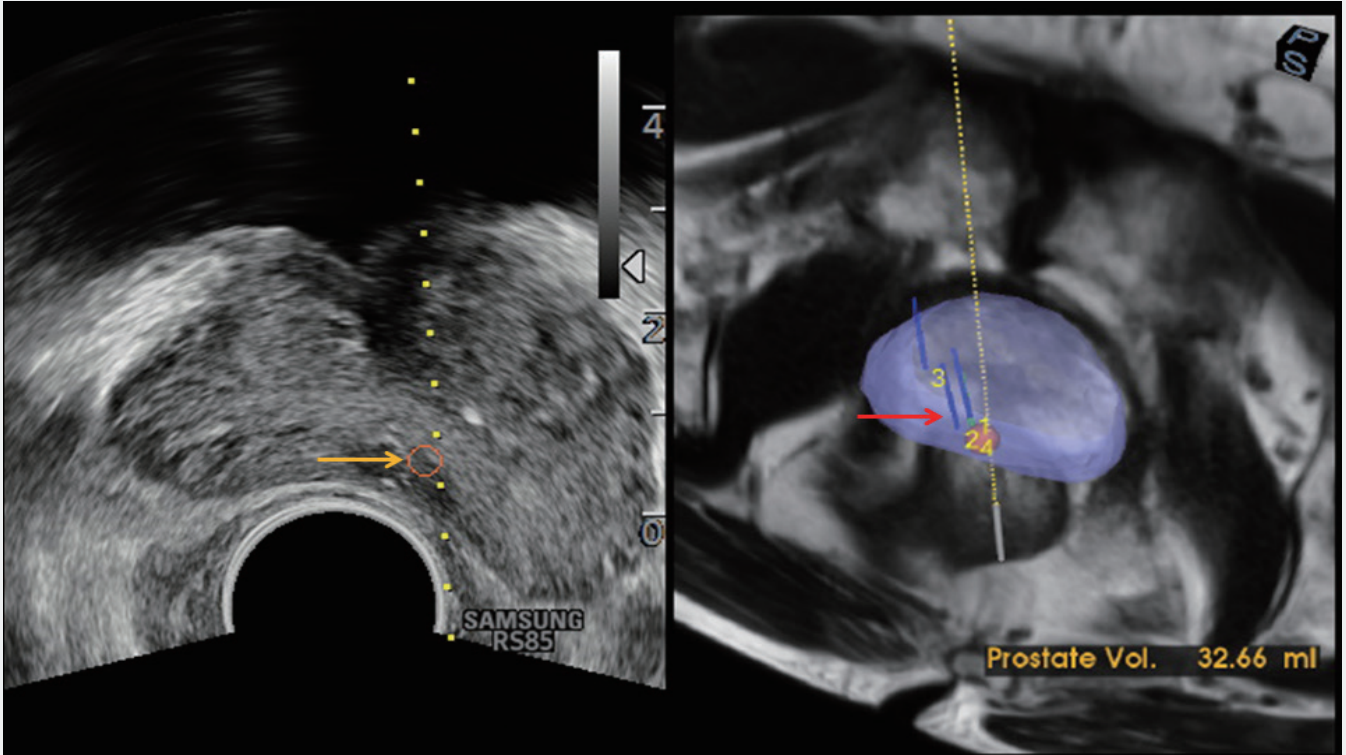


Figure 14. The software for prostate image fusion allows precise targeting of the prostate biopsies based on 3D model. Target lesion marked as a red sphere in MRI and in conventional B-mode (yellow arrow). The already done biopsies are reported in the prostate model (red arrow).

Summary

Up to now, the TRUS-guided 12-position prostate biopsy has been performed as gold standard to confirm the diagnosis of prostate carcinoma. This conventional method is quickly available and cost-effective. New clinical and technical developments in the field of magnetic resonance imaging (MRI) and targeted image-guided biopsy techniques have greatly improved the detection, localization and staging of prostate cancer in recent years [44-45].

The integration of multiparametric MRI (mpMRI), currently the best prostate imaging technique, into the biopsy procedure has led to a significantly increased sensitivity for the detection of clinically significant tumors compared to 12-time TRUS-guided biopsy [40, 46].

Siddiqui et al [40] were able to show in a published cohort of 1003 patients that MRI/TRUS fusion biopsies detect 30% more significant high-risk PCa ($p < 0.001$) and at the same time 17% less insignificant PCa ($p = 0.002$) than conventional biopsies. For the indication of rebiopsy, MRI fusion biopsy has convincingly demonstrated its importance in studies which involved several thousand patients [40, 47-51].

References

1. Robert-Koch-Institut. Prostatakrebs. http://www.krebsdaten.de/Krebs/DE/Content/Krebsarten/Prostatakrebs/prostatakrebs_node.html
2. Herlemann A, Kretschmer A, Apfelbeck M, Tritschler S, Fendler W, Bartenstein P, Reiser M, Stief CG, Gratzke C. Prostate Cancer - Update 2017]. MMW Fortschr Med. 2017 Mar;159(4):58-65
3. Deutsche Gesellschaft für Urologie e. V. (2014) Interdisziplinäre Leitlinie der Qualität S3 zur Früherkennung, Diagnose und Therapie der verschiedenen Stadien des Prostatakarzinoms 2014. Deutsche Gesellschaft für Urologie e. V., Düsseldorf
4. Roethke M1, Anastasiadis AG, Lichy M, Werner M, Wagner P, Kruck S, Claussen CD, Stenzl A, Schlemmer HP, Schilling D. MRI-guided prostate biopsy detects clinically significant cancer: analysis of a cohort of 100 patients after previous negative TRUS biopsy. World J Urol. 2012 Apr;30(2):213-8. doi: 10.1007/s00345-011-0675-2. Epub 2011 Apr 22.
5. Shaw GL, Thomas BC, Dawson SN, Srivastava G, Vowler SL, Gnanapragasam VJ, Shah NC, Warren AY, Neal DE Identification of pathologically insignificant prostate cancer is not accurate in unscreened men. Br J Cancer. 2014 May 13;110(10):2405-11.
6. Siddiqui MM, Rais-Bahrami S, Turkbey B, George AK, Rothwax J, Shakir N, Okoro C, Raskolnikov D, Parnes HL, Linehan WM, Merino MJ, Simon RM, Choyke PL, Wood BJ, Pinto PA Comparison of MR/ultrasound fusion-guided biopsy with ultrasound-guided biopsy for the diagnosis of prostate cancer. JAMA. 2015 Jan 27;313(4):390-7
7. Ukimura O, Coleman JA, de la Taille A, Emberton M, Epstein JI, Freedland SJ, Giannarini G, Kibel AS, Montironi R, Ploussard G, Roobol MJ, Scattoni V, Jones JS Contemporary role of systematic prostate biopsies: indications, techniques, and implications for patient care. Eur Urol. 2013 Feb;63(2):214-30.
8. Eggener SE, Badani K, Barocas DA, Barrisford GW, Cheng JS, Chin AI, Corcoran A, Epstein JI, George AK, Gupta GN, Hayn MH, Kauffman EC, Lane B, Liss MA, Mirza M, Morgan TM, Moses K, Nepple KG, Preston MA, Rais-Bahrami S, Resnick MJ, Siddiqui MM, Silberstein J, Singer EA, Sonn GA, Sprenkle P, Stratton KL, Taylor J, Tomaszewski J, Tollefson M, Vickers A, White WM, Lowrance WT. Gleason 6 Prostate Cancer: Translating Biology into Population Health. J Urol. 2015 Sep;194(3):626-34
9. Lund L, Svolgaard N, Poulsen MH. Prostate cancer: a review of active surveillance. Res Rep Urol. 2014 Aug 16;6:107-12.

10. Hoedemaeker RF et al. Histopathological prostate cancer characteristics at radical prostatectomy after population based screening. *J Urol.* 2000;164:411–5
11. Mottet N et al. EAU-ESTRO-SIOG Guidelines on Prostate Cancer. Part 1: Screening, Diagnosis, and Local Treatment with Curative Intent. *Eur Urol.* 2016.
12. Leitlinienprogramm Onkologie (Deutsche Krebsgesellschaft, Deutsche Krebshilfe, AWMF): Interdisziplinäre Leitlinie der Qualität S3 zur Früherkennung, Diagnose und Therapie der verschiedenen Stadien des Prostatakarzinoms, Kurzversion 3.1, AWMF Registernummer: 043/0220L, <http://leitlinienprogrammmonkologie.de/Leitlinien.7.0.html>
13. Dahnert WF, Hamper UM, Eggleston JC et al. (1986) Prostatic evaluation by transrectal sonography with histopathologic correlation: the echogenic appearance of early carcinoma. *Radiology*158:97-102
14. Shinohara K, Wheeler TM, Scardino PT (1989) The appearance of prostate cancer on transrectal ultrasonography: correlation of imaging and pathological examinations. *The Journal of urology*142:76-82
15. Halpern EJ, Strup SE (2000) Using gray-scale and color and power Doppler sonography to detect prostatic cancer. *AJR. American journal of roentgenology*174:623-627
16. Frauscher F, Klauser A, Halpern EJ (2002) Advances in ultrasound for the detection of prostate cancer. *Ultrasound quarterly*18:135-142
17. Brock M, Von Bodman C, Sommerer F et al. (2011) Comparison of real-time elastography with grey-scale ultrasonography for detection of organ-confined prostate cancer and extra capsular extension: a prospective analysis using whole mount sections after radical prostatectomy. *BJU international* 108:E217-222
18. Lee F, Siders DB, Torp-Pedersen ST et al. (1991) Prostate cancer: transrectal ultrasound and pathology comparison. A preliminary study of outer gland (peripheral and central zones) and inner gland (transition zone) cancer. *Cancer* 67:1132-1142
19. Rorvik J, Halvorsen OJ, Servoll E et al. (1994) Transrectal ultrasonography to assess local extent of prostatic cancer before radical prostatectomy. *British journal of urology* 73:65–69
20. Rosenkrantz AB, Verma S, Turkbey B (2015) Prostate cancer: top places where tumors hide on multiparametric MRI. *AJR* 204(4):W449–W456

21. Fütterer JJ, Briganti A, De Visschere P et al (2015) Can clinically significant prostate cancer be detected with multiparametric magnetic resonance imaging? A systematic review of the literature. *Eur Urol* 68:1045–1053
22. Dickinson L, Ahmed H, Clare A et al (2011) Magnetic resonance imaging for the detection, localisation, and characterisation of prostate cancer: recommendations from a European consensus meeting. *Eur Urol* 59(4):477–494
23. Gupta RT, Spilseth B, Patel N et al (2016) Multiparametric prostate MRI: focus on T2-weighted imaging and role in staging of prostate cancer. *Abdom Radiol* 41(5):831–843
24. Koksall IT, Ozcan F, Kadioglu TC et al (2000) Discrepancy between Gleason scores of biopsy and radical prostatectomy specimens. *Eur Urol* 37(6):670–674
25. Nörenberg D, Solyanik O, Schlenker B, Magistro G, Ertl-Wagner B, Clevert DA, Stief C, Reiser MF, D'Anastasi M. MRI of the prostate *Urologe A*. 2017 May;56(5):665–677.
26. Solyanik O, Schlenker B, Gratzke C, Ertl-Wagner B, Clevert DA, Stief C, Ricke J, Nörenberg D. Imaging of locally advanced prostate cancer : Importance of ultrasound and especially MRI *Urologe A*. 2017 Nov;56(11):1383–1393
27. Barentsz JO, Richenberg J, Clements R, Choyke P, Verma S, Villeirs G, Rouviere O, Logager V, Fütterer JJ; ESUR prostate MR guidelines 2012. *European Society of Urogenital Radiology. Eur Radiol*. 2012 Apr;22(4):746–57
28. Schlenker B, Clevert DA, Salomon G. Sonographic imaging of the prostate *Urologe A*. 2014 Jul;53(7):1052–60
29. Wein W, Brunke S, Khamene A et al. (2008) Automatic CT-ultrasound registration for diagnostic imaging and image-guided intervention. *Medical image analysis* 12:577–585
30. Wein W, Khamene A, Clevert DA et al. (2007) Simulation and fully automatic multimodal registration of medical ultrasound. *Medical image computing and computer-assisted intervention: MICCAI ... International Conference on Medical Image Computing and Computer-Assisted Intervention* 10:136–143
31. Zikic D, Wein W, Khamene A et al. (2006) Fast deformable registration of 3D-ultrasound data using a variational approach. *Medical image computing and computer-assisted intervention: MICCAI ... International Conference on Medical Image Computing and Computer-Assisted Intervention* 9:915–923

32. Clevert DA, Helck A, D'anastasi M et al. (2011) Ultraschallgesteuerte EVAR-Interventionen und Follow-up-Diagnostik mit der kontrastmittelgestützten Sonographie und der Bildfusion. *Gefäßchirurgie* 16:490-497
33. Clevert DA, Helck A, Paprottka PM et al. (2011) Latest developments in ultrasound of the liver. *Der Radiologe* 51:661-670
34. Clevert DA, Helck A, Paprottka PM et al. (2012) [Ultrasound-guided image fusion with computed tomography and magnetic resonance imaging. Clinical utility for imaging and interventional diagnostics of hepatic lesions]. *Der Radiologe* 52:63-69
36. Clevert DA, D'anastasi M, Jung EM (2013) Contrast-enhanced ultrasound and microcirculation: efficiency through dynamics--current developments. *Clinical hemorheology and microcirculation* 53:171-186
37. Clevert DA, Sterzik A, Braunagel M et al. (2013) Modern imaging of kidney tumors. *Der Urologe. Ausg. A* 52:515-526
38. Helck A, Notohamiprodjo M, Danastasi M et al. (2012) Ultrasound image fusion - clinical implementation and potential benefits for monitoring of renal transplants. *Clinical hemorheology and microcirculation* 52:179-186
38. Hadaschik BA, Kuru TH, Tulea C et al. (2011) A novel stereotactic prostate biopsy system integrating pre-interventional magnetic resonance imaging and live ultrasound fusion. *The Journal of urology* 186:2214-2220
39. Siddiqui MM, Rais-Bahrami S, Truong H, Stamatakis L, Vourganti S, Nix J, Hoang AN, Walton-Diaz A, Shuch B, Weintraub M, Kruecker J, Amalou H, Turkbey B, Merino MJ, Choyke PL, Wood BJ, Pinto PA. Magnetic resonance imaging/ultrasound-fusion biopsy significantly upgrades prostate cancer versus systematic 12-core transrectal ultrasound biopsy. *Eur Urol.* 2013 Nov;64(5):713-719.
40. Siddiqui MM, Rais-Bahrami S, Turkbey B, George AK, Rothwax J, Shakir N, Okoro C, Raskolnikov D, Parnes HL, Linehan WM, Merino MJ, Simon RM, Choyke PL, Wood BJ, Pinto PA. Comparison of MR/ultrasound fusion-guided biopsy with ultrasound-guided biopsy for the diagnosis of prostate cancer. *JAMA.* 2015 Jan 27;313(4):390-7
41. Apfelbeck M, Clevert DA, Ricke J, Stief C, Schlenker B. Contrast enhanced ultrasound (CEUS) with MRI image fusion for monitoring focal therapy of prostate cancer with high intensity focused ultrasound (HIFU) *Clin Hemorheol Microcirc.* 2018;69(1-2):93-100

42. Schlenker B, Apfelbeck M, Buchner A, Stief C, Clevert DA. MRI-TRUS fusion biopsy of the prostate: Quality of image fusion in a clinical setting. *Clin Hemorheol Microcirc.* 2018;70(4):433-440.
43. Schlenker B, Apfelbeck M, Armbruster M, Chaloupka M, Stief CG, Clevert DA. Comparison of PIRADS 3 lesions with histopathological findings after MRI-fusion targeted biopsy of the prostate in a real world-setting. *Clin Hemorheol Microcirc.* 2019;71(2):165-170
44. Ahmed HU, El-Shater Bosaily, Brown LC et al (2017) Diagnostic accuracy of multi-parametric MRI and TRUS biopsy in prostate cancer (PROMIS): a paired validating confirmatory study. *Lancet* 389(16):815–822.
45. Graham J, Kirkbride P, Cann Ketal (2014) Prostate cancer: summary of updated NICE guidance. *BMJ* 7524:348
46. Panebianco V, Barchetti F, Sciarra A et al (2015) Multiparametric magnetic resonance imaging vs. standard care in men being evaluated for prostate cancer: a randomized study. *Urol Oncol* 33(1):17.e1–7
47. Kuru TH, Roethke MC, Seidenader J et al (2013) Critical evaluation of magnetic resonance imaging targeted, transrectal ultrasound guided transperineal fusion biopsy for detection of prostate cancer. *J Urol* 190(4):1380–1386
48. Radtke JP, Kuru TH, Boxler S et al (2015) Comparative analysis of transperineal template saturation prostate biopsy versus magnetic resonance imaging targeted biopsy with magnetic resonance imaging-ultrasound fusion guidance. *J Urol* 193(1):87–94
49. Siddiqui MM, Rais-Bahrami S, Truong H et al (2013) Magnetic resonance imaging/ultrasound-fusion biopsy significantly upgrades prostate cancer versus systematic 12-core transrectal ultrasound biopsy. *Eur Urol* 64(5):713–719
50. Valerio M, Donaldson I, Emberton M et al (2014) Detection of clinically significant prostate cancer using magnetic resonance imaging-ultrasound fusion targeted biopsy: a systematic review. *Eur Urol* 65:124–137
51. Distler F, Radtke JP, Kesch C, Roethke M, Schlemmer HP, Roth W, Hohenfellner M, Hadaschik B. Value of MRI/ultrasound fusion in primary biopsy for the diagnosis of prostate cancer. *Urologe A.* 2016 Feb;55(2):146-55

SAMSUNG MEDISON CO., LTD.

© 2020 Samsung Medison All Rights Reserved.

Samsung Medison Reserves the right to modify any design, packaging, specifications and features shown herein, without prior notice or obligation.

Disclaimer

[Do not distribute this document to customers unless relevant regulatory and legal affairs officers approve such distribution.]

- * The features mentioned in this document may not be commercially available in all countries. Due to regulatory reasons, their future availability cannot be guaranteed.
- * Images may have been cropped to better visualize its pathology.
- * This clinical practice review is not an official clinical study or paper presented at a conference. It is a result of a personal study conducted by collaboration between Samsung Medison and Prof. Dirk Clevert. This review is to aid customer in their understanding, but the objectivity is not secured.
- * 본자료는 공식 임상시험 결과물이나 학회에 발표된 논문이 아니며 삼성메디슨이 Dirk Clevert 교수님과 협업하여 산출된 개인 연구의 결과물입니다. 고객의 요청에 따라 이해를 돕기 위해 제공하는 자료일 뿐 객관성은 확보되지 않았습니다.

Please visit <http://www.samsung.com/global/business/healthcare>